*Progress In Electromagnetics Research C, Vol. 23, 161–173, 2011*

# A NOVEL KA-BAND SOLID-STATE POWER COMBINING AMPLIFIER

**L. Zhao***, **J. Xu, L. Wang, and M.-Y. Wang**

School of Physical Electronics, University of Electronic Science and Technology of China, Chengdu 610054, China

**Abstract**—This paper presents a high-efficiency Ka-band solid-state power combining amplifier on the basis of a novel waveguide magic tee. By employing 16 low-power amplifier modules and compact waveguide power combining network with a low loss microstrip-to-waveguide transition, the output loss of the combining circuit is minimized, so a high combining efficiency larger than 85% from 34 to 36 GHz is obtained. Modular architecture is adopted in the combiner design. The single amplifier, bias circuit and heat sink are all fabricated separately, which add great flexibility to the system. Modular amplifiers can be premade and reserved in case any malfunctioning amplifier needs to be replaced. In addition, the improved power combining amplifier has the advantages of low loss, high isolation, compact structure, excellent heat-sink, etc.

## 1. INTRODUCTION

The power amplifier is a key part in high frequency communication system. It is not only widely used in commercial wireless communication base stations, but also extensively used in military electronic reconnaissance, jamming, radar, guidance, etc. [1–5]. Currently, applying vacuum devices especially traveling wave tubes can obtain relatively higher power output. But there exist perplexed power supply, high spurious and serious distortion when the devices achieve saturated output power. Solid-state amplifier is to become a better choice in low and medium power applications [1, 6]. Compared with traditional power vacuum transmitters, solid-state transmitters have the advantages of high gain, low noise, small size, lower operating voltage, no warm-up time, etc. [2, 7]. However, the output

*Received 14 June 2011, Accepted 3 August 2011, Scheduled 16 August 2011*
* Corresponding author: Li Zhao (niuniuwanglei@126.com).

power of single solid-state devices cannot meet the needs of the engineering. Power-combining technologies have been proposed [4, 8]. When combining a large number of monolithic microwave integrated circuits (MMIC) to form a solid-state amplifier, the system efficiency is determined primarily by the loss of the output combiner [6, 9].

Thus, a low loss combining method is needed for corporate combining. Power splitters are used as input and output ports of combining network in the design of power amplifier. Its performance of broadband, high-capacity and low insertion loss directly determines the quality of the whole system [10, 11]. Conventional integrated planar transmission line power divider has the advantages of small size and low cost, but it also has the disadvantage of big-loss, poor-isolation and limited-power capacity [6–8]. Although the array-spatial power combining with the advantages of high efficiency and small size, it faces serious heat problem. The closer the amplification units are from the center, the higher their temperature will be, which restricts its application. Ordinary E-T power divider has a lower isolation between the two ports. 3 dB waveguide direction coupler splitter is large in size and requires high accuracy in the processing [9]. Since the synthetic efficiency of some other traditional methods of power combining, such as Wilkinson power splitter, Lange bridge and branch line coupler etc., decreases significantly with increased stages, they are generally not more than two stages in the practical application. In summing up the advantages and disadvantages of the power splitter mentioned above, this paper proposes a new type of waveguide magic tee splitter and a compact millimeter-wave solid-state power combining scheme.

## 2. NOVEL MAGIC TEE POWER SPLITTER

### 2.1. Theory

The common 3-port network such as Wilkinson bridge, waveguide $T$-junction and waveguide-microstrip dual-probe power combiner cannot match three ports perfectly at the same time according to the network theory. If working out a compromise between port reflection and isolation to minimize $S_{11}$, the ideal values of scattering parameters can be obtained:

$$[S] = \begin{bmatrix} S_{11} & S_{12} & S_{13} \\ S_{21} & S_{22} & S_{23} \\ S_{31} & S_{32} & S_{33} \end{bmatrix} = \begin{bmatrix} 0 & \sqrt{2}/2 & \sqrt{2}/2 \\ \sqrt{2}/2 & S_{22} & S_{23} \\ \sqrt{2}/2 & S_{32} & S_{33} \end{bmatrix} \tag{1}$$

where

$$|S_{22}|^2 + |S_{23}|^2 + 0.5 = 1 \tag{2}$$

So that,

$$S_{22} = S_{33} = S_{32} = S_{23} = \ -6 \text{ dB} \tag{3}$$

Then, it can obtain only $-6$ dB isolation of the 3-port network.

The ideal magic tee is a lossless, reciprocal four-port network and constituted of waveguide double-T and matching components. The double-T is composed of $E$-$T$ and $H$-$T$ joints as shown in Fig. 1(a). It can be seen from the symmetry and isolation property of the structure that the scattering parameters of the double-T meet the following relationship:

$$S_{13} = S_{23}, \quad S_{14} = -S_{24}, \quad S_{11} = S_{22} \tag{4}$$

Then taking into account the reciprocity, scattering matrix can be

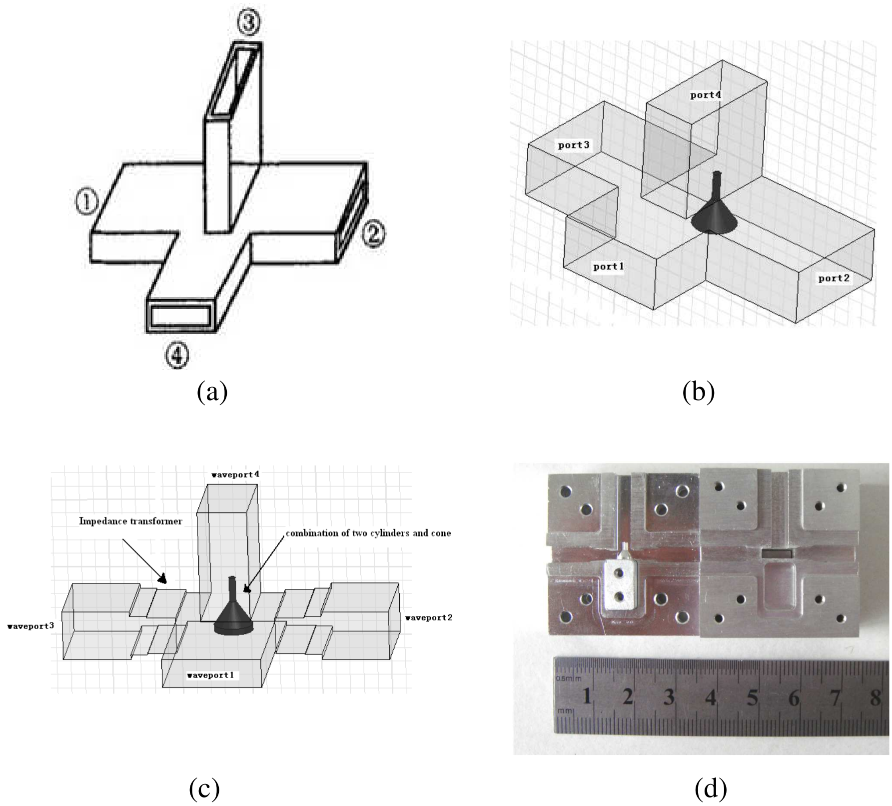


**Figure 1.** Model of the 2-way combiner, (a) waveguide double-T, (b) typical deployment structure, (c) the novel structure, (d) the photo.

written as:

$$[S] = \begin{bmatrix} S_{11} & S_{12} & S_{13} & S_{14} \\ S_{21} & S_{22} & S_{23} & S_{24} \\ S_{31} & S_{32} & S_{33} & S_{34} \\ S_{41} & S_{42} & S_{43} & S_{44} \end{bmatrix} = \begin{bmatrix} S_{11} & S_{12} & S_{13} & S_{14} \\ S_{12} & S_{11} & S_{13} & -S_{14} \\ S_{13} & S_{13} & S_{33} & 0 \\ S_{14} & -S_{14} & 0 & S_{44} \end{bmatrix} \tag{5}$$

Ports 3 and 4 can achieve perfect match by adding the matching components, then

$$S_{33} = S_{44} \tag{6}$$

For lossless structures, it can prove that,

$$S_{11} = S_{22} \tag{7}$$

In this case, it is called matching double-T, which is the magic tee. The scattering matrix can be written as:

$$[S] = \begin{bmatrix} S_{11} & S_{12} & S_{13} & S_{14} \\ S_{12} & S_{11} & S_{13} & -S_{14} \\ S_{13} & S_{13} & 0 & 0 \\ S_{14} & -S_{14} & 0 & 0 \end{bmatrix} \tag{8}$$

Suppose magic tee is a lossless network. It follows Equation (9) according to energy conservation law.

$$[S]\,[S^*] = [E] \tag{9}$$

So, the scattering matrix can be calculated as follow:

$$\begin{cases} |S_{41}|^2 + |S_{41}|^2 = 1 \\ |S_{41}|^2 + |S_{11}|^2 + |S_{12}|^2 + |S_{13}|^2 = 1 \\ |S_{41}|^2 + |S_{12}|^2 + |S_{22}|^2 + |S_{13}|^2 = 1 \\ |S_{13}|^2 + |S_{13}|^2 = 1 \end{cases} \tag{10}$$

Thus we have:

$$\begin{cases} |S_{11}|^2 + |S_{12}|^2 = 1 \\ |S_{12}|^2 + |S_{22}|^2 = 1 \end{cases} \tag{11}$$

Finally, the scattering matrix is expressed as:

$$[s] = \frac{1}{\sqrt{2}} \begin{bmatrix} 0 & 0 & 1 & 1 \\ 0 & 0 & -1 & 1 \\ 1 & -1 & 0 & 0 \\ 1 & 1 & 0 & 0 \end{bmatrix} \tag{12}$$

It can be seen that when ports 3 and 4 are matched perfectly, ports 1 and 2 can achieve not only automatical matching, but also good isolation. This property of the magic tee splitter mentioned above makes achieving high isolation and ideal match much easier than a single *E*-*T* or *H*-*T* junction.

## 2.2. Model

The above analysis shows that the incident energy of port 1 through the electric field coupled to the magic tee can be equivalent to capacitive coupling, while the energy of port 4 through the magnetic field coupled to the magic tee is equivalent to inductive coupling, so $E$-arm must be deployed by inductive components, and $H$-arm be deployed by capacitive elements. For this purpose, the cone-shaped tuning bar is often adopted, shown in Fig. 1(b). This method can achieve good matching and isolation between ports 1 and 4. However, the bandwidth is not wide, while the isolation of two equal arms can only reach 15 dB. The design is improved in the following. Tuning rod must present inductance characteristics to the $E$-arm, while presenting capacitance characteristics to the $H$-arm in order to deploy $E$-arm and $H$-arm simultaneously. The combination of two cylinders and cone in the new structure provides capacitance characteristics for matching the $T$-branch waveguide of $H$-plane. Taking into account the metal cylindrical surface will result in unnecessary reflection for the matching of $T$-branch waveguide of $E$-plane, also the new structure can provide the required capacitive properly for matching it, at the same time inhibit the reflex of $E$-arm. In order to widen the bandwidth, we compress the height of two branches of the $H$ plane $T$-junction to reduce the cutoff wavelength of electromagnetic waves transmitting in it. As a result, the model of the novel structure shown in Fig. 1(c) and Fig. 1(d) is the final 2-way magic tee combiner.

## 2.3. Results

Both the simulated and measured results of the 2-way magic tee combiner are depicted in Fig. 2. The simulated curves indicate that the isolation between the two ports is better than 20 dB, that insertion loss is less than 0.02 dB, and that return loss is better than 25 dB from 32 to 36 GHz, while the measured curves show that insertion loss is less than 0.15 dB, that return loss is better than 22 dB, and that the isolation between the two ports is better than 18 dB. An obvious difference is shown between the two results, although the absolute amount of change is still very small. Therefore, it is believed that the differences shown in Figs. 2(a) and 2(b) comes from conductor loss which was not considered in calculation. Of course, other losses of manufacture precision also exist, such as minor variances of waveguide width or height, a little warp between port 1 and 2, etc., which result in other differences between simulated and measured results. The differences shown in Fig. 2(c) are mainly because the reflected wave is not completely absorbed by absorption port, which results from

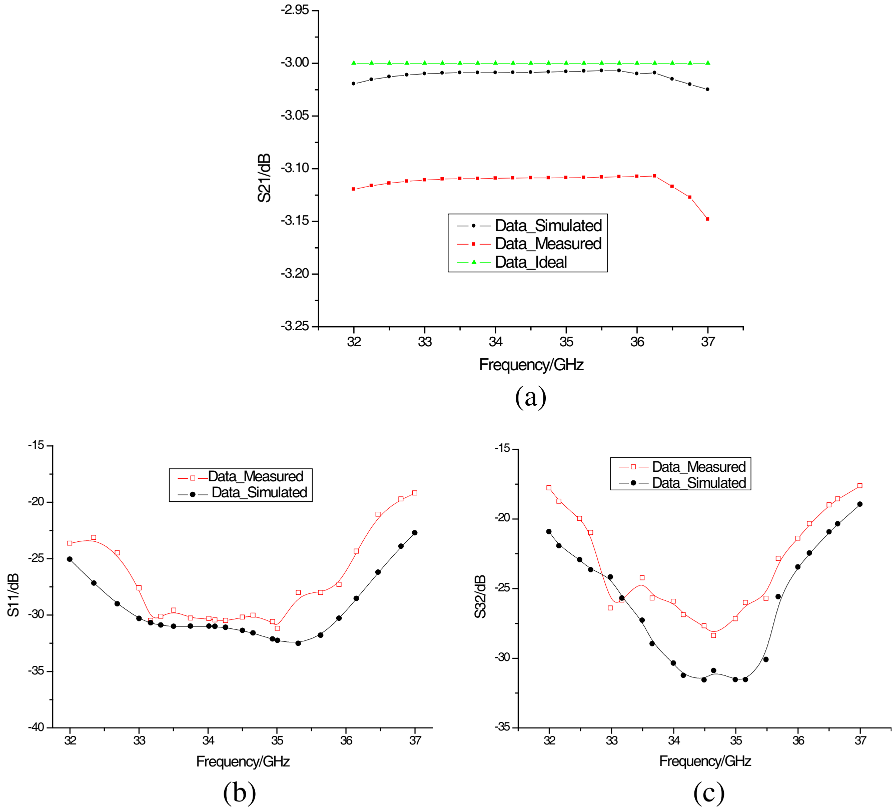


**Figure 2.** The performances of the 2-way magic tee splitter, (a) insertion loss, (b) return loss, (c) isolation.

pasting microwave absorbing material not using standard matching load in port 4. The indexes of the structure are better than traditional structure. Especially in terms of isolation, it is far superior to traditional *E*-*T* power divider.

## 3. COMBINING NETWORK

### 3.1. 16-way Amplifier Power Combining Scheme

Figure 3 shows that *H* plane directional coupler combines 14 W by 2 ways 7.5 W module. The 7.5 W module is achieved with magic tee, 8-way splitter/combiner and 8 ways 1 W module. The advantages of this scheme are that each module fits into the cavity after debugged to identical in power and phase which facilitate the whole debugger and

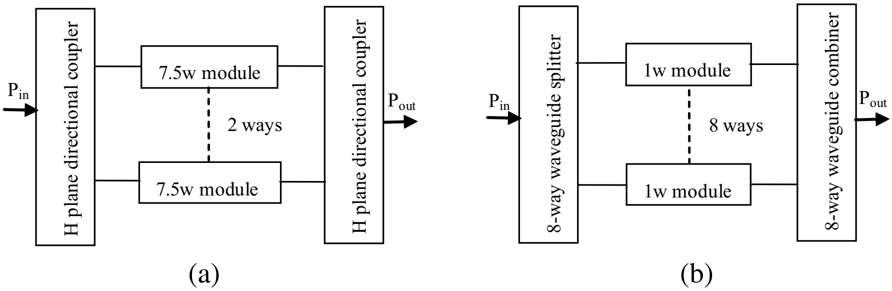


**Figure 3.** The functional block diagram of the 16-way power amplifier, (a) 14 W module, (b) 7.5 W module.

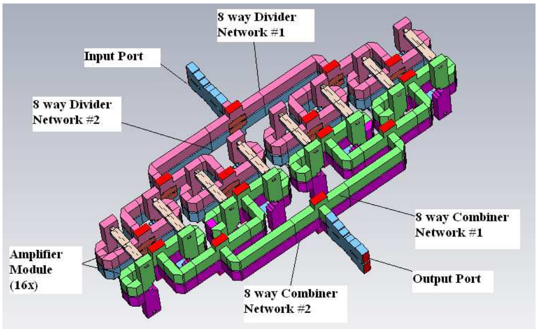


**Figure 4.** The simulation model of the 16-way power amplifier.

that the 1 W module is in small size and simple structure.

The whole network is a split-block multilayer design. The waveguide layout consists of three layers of copper with the middle layer having two sides, which reduces the volume greatly. The final dimensions are 54 mm (height) × 183 mm (length) × 95 mm (wide). Dimensions are optimized using a mixture of full-wave and circuit modules to provide reflection and isolation approaching 25 dB across the band to minimize amplitude and phase ripple. The simulation model is shown in Fig. 4.

### 3.2. Measurement of the Splitter/combiner Loss

Figure 5 shows the measured transmission coefficients for all 16 paths in the combiner. The ideal 16-way split amplitude near −12 dB is shown, along with the ideal value reduced by the design requirement of 1 dB insertion loss across the band. The measured data show an average insertion loss of approximately 0.8 dB, well within the

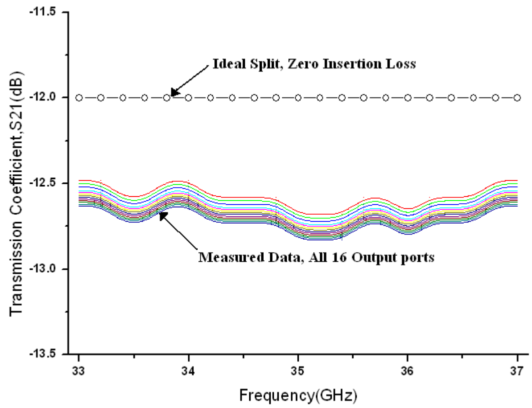


**Figure 5.** Measured insertion loss of the splitter/combiner.

requirement, giving a power combining efficiency $> 85\%$. The insertion loss includes (1) waveguide losses which made from the material copper, (2) processing losses as the smaller waveguide size in the 8 mm band and complex structure of the waveguide combiner have a higher requirement on manufacture and installation, (3) measurement losses come from instrument calibration and waveguide adapter. The result is a compact highly efficient combiner that provides a 16-way split of an amplified input signal and a 16-way recombination of these high power signals to provide a saturated output power of 14 W with module powers in the 2 W range. Comparison of other waveguide combiners in this frequency range would include the dual-probe combiner [12], which has average loss of 0.4 dB over the band while combining 4 ports and not offering port-to-port isolation.

## 4. 16-WAY HIGH POWER COMBINING AMPLIFIER

### 4.1. Low Loss Microstrip-to-waveguide Transition

In order to avoid additional output loss in the combiner, it is necessary to minimize the insertion loss from the microstrip (output of the packaged MMIC) to the waveguide (input of the combiner/divider), so as not to reduce power combining efficiency of the overall system [13, 14]. Therefore, the design of the microstrip-to-waveguide transition must be considered as designing the system. An $E$-field probe transition in view of engineering requires is given in Fig. 6(a). The key elements that affect performance of the transition are length, width of the probe inserted into the waveguide and distance between

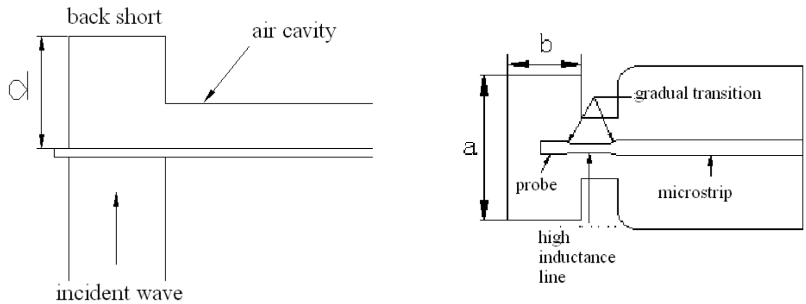


(a)

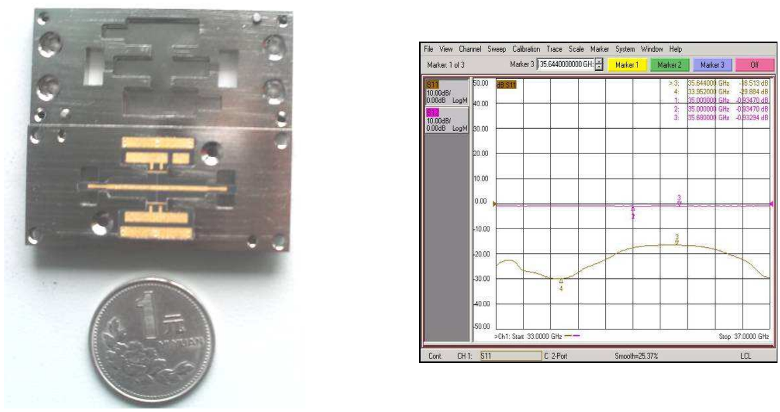

(b)

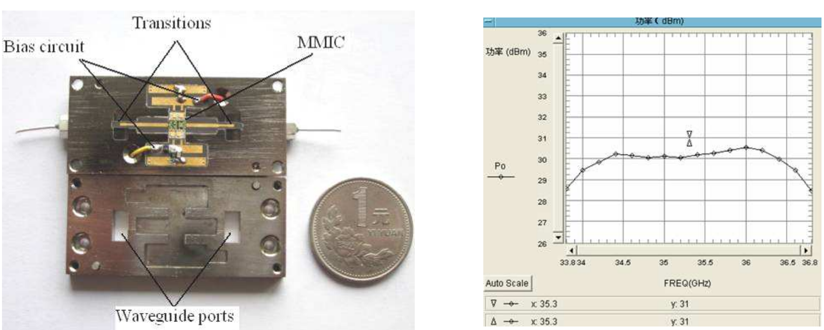


(c)

**Figure 6.** Microstrip-to-waveguide transition, (a) structure, (b) back-to-back transitions and test results, (c) single amplifier and measured $P_o$.

probe and short-road surface [13]. Slight changes of the dimensions will cause the performances of the probe transition to deteriorate extremely. Fig. 6(b) indicates that the back-to-back transitions without chip has a return loss better than 16 dB and insertion loss less than 1 dB (including microstrip loss 0.4 dB, so the insertion loss of the single transition is less than 0.3 dB). Fig. 6(c) shows that the output power of the single amplifier module is approximately 30 dBm over 34–36 GHz.

## 4.2. Chip Selection

We select GaAs MMIC power amplifier chip NC1188C-3436 provided by China Electronics Technology Corporation No. 13 (CETC 13). It is a millimeter-wave high-power amplifier chip covering 34–36 GHz, with power gain of 16 dB, saturated output power ($P_o$) of 30 dBm, power added efficiency (PAE) of 28% as shown in Fig. 7.

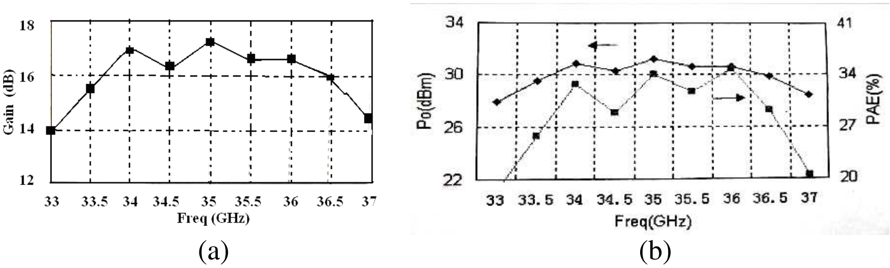


**Figure 7.** Parameters of the chip, (a) power gain, (b) $P_o$ and PAE.

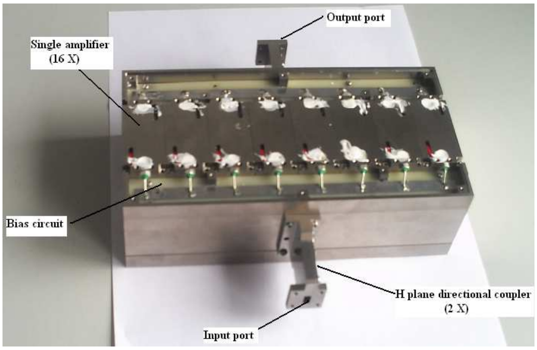


**Figure 8.** 16-way power amplifier with bias circuit.

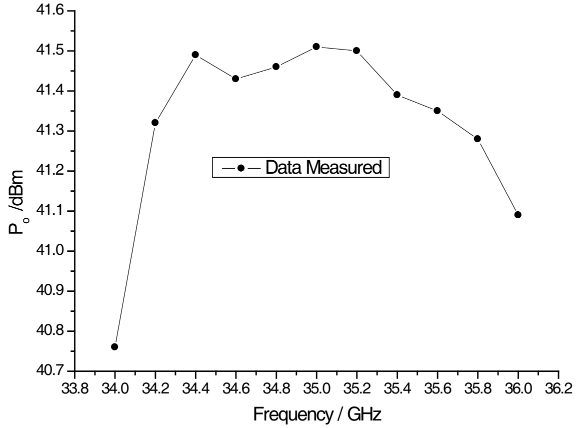


**Figure 9.** Measured $P_o$ of the 16-way power amplifier.

### 4.3. Characterization of 16-way Power Amplifier

A 16-way high power combining amplifier is fabricated, as shown in Fig. 8. The single amplifier, bias circuit and heat sink are all fabricated separately. Furthermore, the driving stage is fabricated in an independent chamber in order to facilitate testing, debugging and maintenance. The measured $P_o$ of the 16-way power amplifier are shown in Fig. 9, which shows the maximum $P_o$ of the amplifier can achieve 41.51 dBm. Finally, the maximum combining efficiency is 87%, and the average PAE is 25%.

## 5. CONCLUSION

In this paper, a Ka-band solid-state power amplifier has been designed and fabricated with a novel waveguide magic tee. The measured $P_o$ is more than 40.76 dBm. The highest $P_o$ is 41.51 dBm (14 W) at 35 GHz. The combining efficiency is more than 85% from 34 to 36 GHz. This new power combining scheme completed with each module designed individually has properties of low loss, high isolation, compact structure, convenient fabrication process, good heat sinking, and high combining efficiency in a broad band. It can find solutions to the problems swiftly by replacing single module when the system is out of order, which can be competitive with recently published high frequency amplifiers. Such characteristics demonstrate that the proposed power amplifier has strong potential for higher power and higher frequency.

## REFERENCES


1. Epp, L. W., D. J. Hoppe, A. R. Khan, and S. L. Stride, "A high-power Ka-band (31–36 GHz) solid-state amplifier based on low-loss corporate waveguide combining," *IEEE Trans. Microwave Theory Tech.*, Vol. 56, 1899–1908, 2008.
2. Simons, R. N., E. G. Wintucky, J. D. Wilson, and D. A. Force, "Ultra-high power and efficiency space traveling-wave tube amplifier power combiner with reduced size and mass for NASA missions," *IEEE Trans. Microwave Theory Tech.*, Vol. 57, 582-588, 2009.
3. Delisio, M. P. and R. A. York, "Quasi-optical and spatial power combining," *IEEE Trans. Microwave Theory Tech.*, Vol. 50, 929–936, 2002.
4. Chang, K. and C. Sun, "Millimeter-wave power-combining techniques," *IEEE Trans. Microwave Theory Tech.*, Vol. 83, 91–107, 1983.
5. Zhang, B., Y.-Z. Xiong, L. Wang, S. Hu, T.-G. Lim, Y.-Q. Zhuang, and L.-W. Li, "A D-band power amplifier with 30-GHz bandwidth and 4.5-dBm $P_{sat}$ for high-speed communication system," *Progress In Electromagnetics Research*, Vol. 107, 161–178, 2010.
6. Wong, S.-K., F. Kung, W. Lee, S. Maisurah, and M. N. B. Osman, "A wimedia compliant CMOS RF power amplifier for Ultra-wideband (UWB) transmitter," *Progress In Electromagnetics Research*, Vol. 112, 329–347, 2011.
7. Khan, P., L. Epp, and A. Silva, "A Ka-band wideband-gap solid-state power amplifier: Architecture identification," *JPL, Pasadena, CA, Interplanetary Network Progress Rep.*, Vol. 42–162, 1–16, 2005.
8. Buoli, C., S. Fusaroli, V. M. Gadaleta, F. Morgia, and T. Turillo, "Microstrip to waveguide 3 dB power splitter/combiner on FR4 PCB up to 50 GHz," *2005 European Microwave Conference*, 4–6, 2005.
9. Wang, L., J. Xu, L. Zhao, D. Ran, and M. Y. Wang, "A millimeter-wave solid-state power combining circuit based on branch-waveguide directional coupler," *Proceedings 2010 International Symposium on Signals, Systems and Electronics*, Vol. 1, 265–267, 2010.
10. Russell, K. J., "Microwave power combining techniques," *IEEE Trans. Microwave Theory Tech.*, Vol. 27, 472–478, 1979.

11. Wu, H. and W.-B. Dou, "A rigorous analysis and experimental researches of waveguide magic tee at W band," *Progress In Electromagnetics Research*, Vol. 60, 131–142, 2006.
12. Xie, X. Q., C. X. Zhao, and R. Diao, "A millimeter-wave power combining amplifier based on a waveguide-microstrip $E$-plane dual-probe four-way power combining network," *Int. J. Infrared Milli. Waves*, Vol. 29, 862–870, 2008.
13. Aliakbarian, H., A. Enayati, G. A. E. Vandenbosch, and W. de Raedt, "Novel low-lost end-wall microstrip-to-waveguide splitter transition," *Progress In Electromagnetics Research*, Vol. 101, 75–96, 2010.
14. Costanzo, S., "Synthesis of multi-step coplanar waveguide-to-microstrip transition," *Progress In Electromagnetics Research*, Vol. 113, 111–126, 2011.